Journal of Power Sources 254 (2014) 224–231

Contents lists available at ScienceDirect

Journal of Power Sources

journal homepage: www.elsevier.com/locate/jpowsour

Characterisation of embroidered 3D electrodes by use of anthraquinone-1,5-disulfonic acid as probe system

Noemí Aguiló-Aguayo, Thomas Bechtold*

Institute for Textile Chemistry and Textile Physics, Leopold-Franzens-University Innsbruck, Hoechsterstrasse 73, A-6850 Dornbirn, Austria

HIGHLIGHTS

- 100 cm^2 embroidered 3D porous electrode design can be used for electrochemical applications.
- $AQDS^{2-}$ exhibits quasi-reversible consecutive two electron transfer reactions.
- 3D electrode shows current densities similar to micro cell and 100 cm^2 plane Cu-plate electrode.
- 3D electrode presents higher peak-to-peak separation due to its porous nature.

GRAPHICAL ABSTRACT

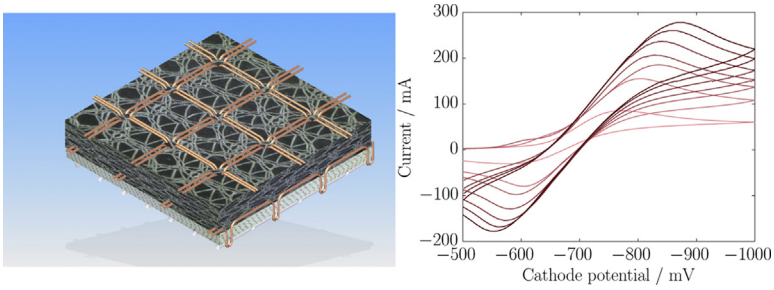

ARTICLE INFO

Article history:
Received 7 August 2013
Received in revised form
13 November 2013
Accepted 19 December 2013
Available online 2 January 2014

Keywords:
Anthraquinone
Porous electrodes
Embroidery
Electrochemistry

ABSTRACT

New electrode designs are required for electrochemical applications such as batteries or fuel cells. Embroidered 3D Cu porous electrodes with a geometric surface of 100 cm^2 are presented and characterised by means of the anthraquinone-1,5-disfulfonic acid ($AQDS^{2-}$) redox system in alkaline solution. The electrochemical behaviour of the 3D electrode is established by the comparison of cyclic voltammetry responses using a micro cell and a 100 cm^2 plane Cu-plate electrode. Dependencies of the peak currents and peak-to-peak potential separation on scan rate and $AQDS^{2-}$ concentration are studied. The $AQDS^{2-}$ characterisation is also performed by means of spectroelectrochemical experiments.

1. Introduction

For many applications of electrochemical energy storage the maximum cell current and energy efficiency are limited by the current density at the electrode. As the composition of the electrolyte and the type of electrode reaction are defined by the type of electrochemical system to be used, an increase in cell current per geometric area requires the use of electrodes with high specific surface.

In particular for application in energy storage different approaches have been chosen to realise a 3D-structured electrodes.

Besides incorporation of conductive fibres into the active electrode coating, three-dimensional structures formed by fibre webs, fabric from conductive material and metal foam have been proposed to increase electrode thickness. The use of a third dimension in the electrodes provides a foundation for the design of different cell configurations and provides enhanced energy efficiency essential in storage energy devices, such as batteries [1].

Embroidery techniques can be useful to prepare conductive 3D-structures for electrodes with high flexibility in geometry and choice of conductive material e.g. Cu-wire, stainless steel fibre yarn, aluminium wires. This allows design of new 3D-current collectors

* Corresponding author.
E-mail addresses: textilchemie@uibk.ac.at, noeaguilo@gmail.com (T. Bechtold).

0378-7753/$ – see front matter © 2014 Elsevier B.V. All rights reserved.
http://dx.doi.org/10.1016/j.jpowsour.2013.12.096

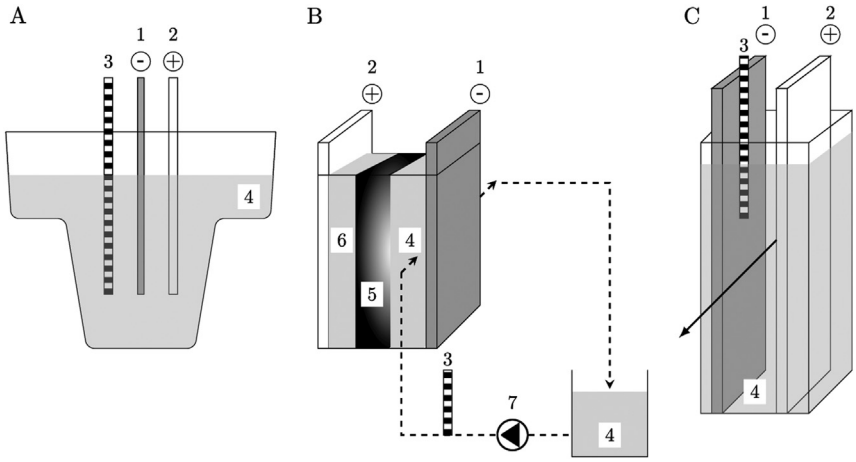

Fig. 1. Schematic drawing of the different cell configurations used in the experiments: 1 cathode, 2 anode, 3 reference electrode, 4 $AQDS^{2-}$ solution. (A) Small cell using circular plane (φ = 1.5 mm in diameter) Cu electrode. (B) 100 cm^2 cell assemblies for the Cu-plate and 3D embroidered Cu porous electrodes: 5 membrane, 6 anolyte, 7 peristaltic pump (arrow indicates the flow direction). (C) Cell for the spectroelectrochemical measurements (arrow indicates the direction of the light beam).

with high conductivity and adjustable porosity. Furthermore when using this technique the electrodes are manufactured in the dimensions of the electrochemical cell and thus no cutting is required. This helps to minimises the risk of short-circuits and hot-spots at the sides of the electrodes.

The electrochemistry of anthraquinoid compounds is of growing interest as the properties of these chemicals makes them interesting for many applications, e.g. oxygen reduction [2–4] hybrid capacitors [5], batteries [6], liquid crystalline applications [7].

The cathodic reduction of anthraquinoid compounds to the dihydroxy form requires the transfer of two electrons. In aprotic solvents radical intermediates can be observed, while in alkaline aqueous solutions a rapid two electron transfer is observed. Depending on the solution's pH value the reduction also involves protonation steps. The anthraquinone-1,5-disulfonate ($AQDS^{2-}$) is a water soluble molecule which exhibits a reversible redox behaviour in alkaline solutions as both the anthraquinone and the reduced leuco form are chemically stable. Thus this compound can serve as soluble redox probe, which can be used to assess performance of electrodes. In addition yellow anthraquinone changes its colour during reduction from yellow to dark red, which allows optical monitoring of the reduction.

In the present work alkaline solutions of $AQDS^{2-}$ were used to characterise the performance of embroidered 3D-electrodes manufactured from Cu-wire. The electrodes were tested by voltammetry in a stopped-flow cell. For comparison CV-experiments with $AQDS^{2-}$ were performed on small diameter plane Cu electrodes, on a 100 cm^2 plane Cu metal electrode and on embroidered 3D-electrodes both mounted in a stopped-flow cell. For further characterisation of the $AQDS^{2-}$ system spectroelectrochemical experiments were performed.

2. Experimental

The redox system under study was a set up of different concentrations (0.005 M, 0.010 M and 0.015 M) of a solution of 9,10-anthraquinone-1,5-disulphonic acid ($AQDS^{2-}$, 95%, Sigma–Aldrich Chemie GmbH, Steinheim, Germany) in 0.1 M NaOH. The electrochemical reduction of $AQDS^{2-}$ was investigated by cyclic voltammetry using three different cell configuration (Fig. 1, Table 1). Cyclic voltammograms (CV) were performed using a potentiostat (EG&G 274A Princeton Applied Research). All potential values were taken related to (Ag/AgCl/3 M KCl) reference electrode (RE).

The micro cell configuration consisted of a small cell (EG&G Mirco Cell, 10 mL catholyte volume), using a circular plane copper working electrode (WE) with 1.5 mm in diameter. The counter electrode (CE) was a Pt-wire electrode placed in a separated electrolyte bridged by a porous diaphragm (vycor). The WE was polished before an experiment by use of a 0.5 μm alumina dispersion (EG&G polishing kit). CV were recorded in the potential range between −500 mV and −850 mV at different scan rates from 5 to 100 mV s^{-1}. Solutions were degassed with argon for 3 min before each CV measurement. Experiments were repeated 5 times for each condition.

The 100 cm^2 cell assemblies were built as parallel plate cell, with anolyte and catholyte separated by a cation-exchange membrane (Nafion type). A plane copper plate with an active area of about 100 cm^2 (mass around 50.14 g/100 cm^2) or an embroidered three-dimensional copper based porous electrode (mass around 4.33 g/100 cm^2) were used as WE [8]. For comparison a 0.1 mm Cu foil with an area of 100 cm^2 would have a mass of 8.61 g/100 cm^2. The schematic presentation of the cross section is given in Fig. 2. The 3D electrodes (Fig. 3) were prepared by technical embroidery (Tegra 71

Table 1
Characteristics of the different cell configurations used. Electrodes present same geometric ($Area_{geom}$) and electrode ($Area_{electr}$) area unless otherwise specified.

Cell configuration	Cathode (WE)	WE dimensions	Anode (RE)	Electrolyte V mL^{-1}
A	Circular Cu-plane	ϕ: 1.5 mm Area: ~1.8 mm^2	Pt wire	10
B	Plane Cu-plate	Area: 100 × 100 mm^2	Stainless steel plate	Anolyte: 300 Catholyte: 800
B	Embroidered 3D Cu porous	Cu-wire ϕ: 0.08 mm Cu-wire length (l): 100 mm Number of wires (N): 400 $Area_{geom}$: 100 × 100 mm^2 $Area_{electr}$: $2\pi(/2)lN = 10^4$ mm^2	Stainless steel plate	Anolyte: 300 Catholyte: 800
C	Plane Cu	Area: 30 × 10 mm^2	Pt foil	2.70

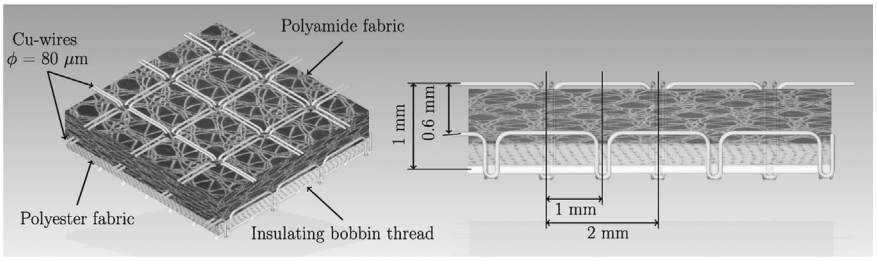

Fig. 2. Schematic overview of the embroidered 3D Cu porous electrode used. Right image corresponds to the section view drawing. Details of the layers are also specified.

Grabher GmbH, Lustenau, Austria). A stainless steel plate of 100 cm^2 active area was used as a CE (anode). The anolyte consisted of 300 mL 0.1 M NaOH solution and a reservoir of 800 mL $AQDS^{2-}$ solution was used as catholyte. For CV measurement the electrolyte flow of the catholyte was stopped. Between repetitive measurements the catholyte was circulated by means of a peristaltic pump in order to refresh the solution inside the cell (flow 200 mL min^{-1}). To achieve a complete penetration of the electrolyte into the structure of the 3D-electrode 1 mL of wetting agent (Primasol®NF, alkyl phosphate, BASF, Ludwigshafen, Germany) was added to 800 mL $AQDS^{2-}$ solution. Further details about the cell assembly are described elsewhere [9]. After an equilibrium time of 60 s at −500 mV the CV were measured in the potential interval between −500 mV and −1000 mV at different scan rates (from 1 to 50 mV s^{-1}). At scan rates higher than 10 mV s^{-1}, a second cycle of the CV was required to minimize disturbing effects due to oxygen reduction during the initial scan and to remove possible Cu-oxides on the electrode surface by cathodic reduction. In addition, equilibrium conditions (−500 mV for 180 s) were applied in order to minimise peak contributions in the spectra due to copper oxides. Experiments were repeated at least three times for each condition.

The plane copper electrode was cleaned before each experiment by polishing with sandpaper to obtain a fresh surface. 3D electrodes were pre-cleaned in a solution of 1.9 g L^{-1} wetting agent (Primasol®NF, alkyl phosphate) and 3.6 g L^{-1} surfactant agent (Kieralon Jet B, non-ionic detergent, BASF, Ludwigshafen a. R., Germany) at 50–60 °C for 25 min, then the electrodes were rinsed with tap water and deionised water. To assure complete removal of any mobile ions e.g. residual water hardness and eventually formed copper-oxides from the 3D-electrode a two stage treatment was applied. After each experiment, 3D electrodes were cleaned firstly with a stirring solution of 10 g L^{-1} citric acid for at least 30 min, then rinsed with deionised water and finally cleaned with a stirring solution of 10 g L^{-1} complexing agent (Trilon A, nitrilo-triacetic acid sodium salt solution, BASF, Ludwigshafen a. R., Germany) for 48 h and rinsed with deionised water.

For the spectroelectrochemical experiments a special cell was designed to record changes in the absorbance near the electrode surface by photometry. It consisted of a cathode based on a copper foil (99.7% purity, 0.1 mm thickness, Merck Darmstadt, Germany) of about 1 cm width, fitted into a 10 mm optical cuvette made from plastic. The cathode surface was oriented parallel to the direction of the light beam, in a position, that the light passes through the diffusion layer established at the front of the cathode. The anodic surface was a platinum foil of about 2 mm in width, mounted outside the light beam of the photometer. The reference electrode was placed inside the plastic cuvette (5 mL) between the copper and the platinum foil. An electrolyte volume of 2.70 mL was used. CV were recorded from −500 mV to −850 mV at 5, 10 and 20 mV s^{-1}. Before each experiment, the copper foil was first cleaned

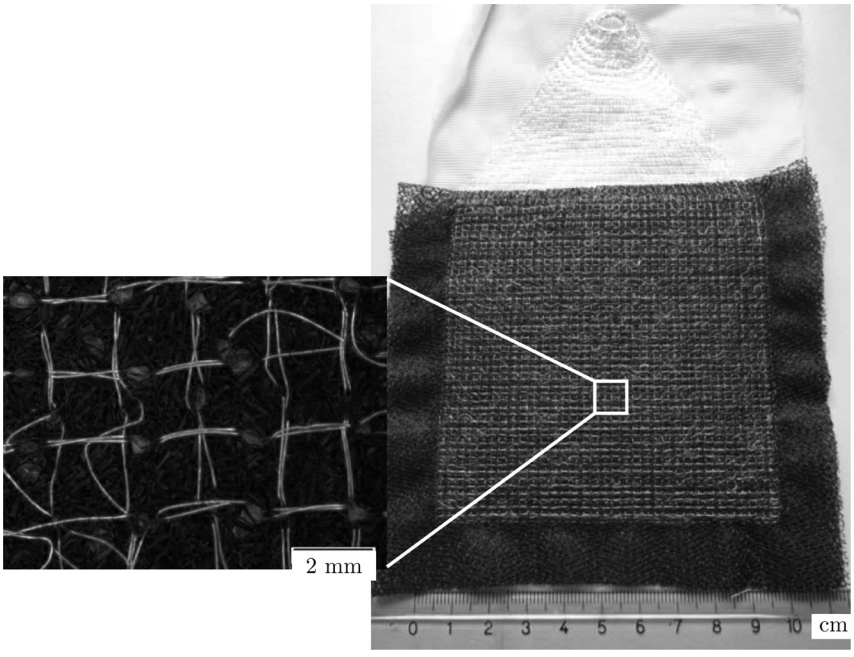

Fig. 3. Embroidered 3D Cu porous electrode used in the experiments (right image) and corresponding optical microscope picture (left image).

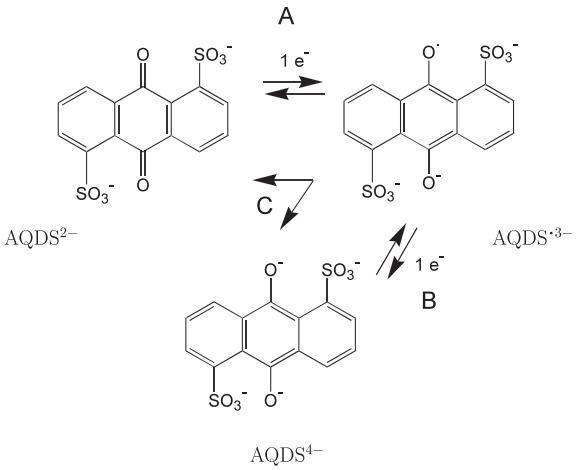

Fig. 4. Overall cathodic reduction of $AQDS^{2-}$ in 0.1 M NaOH (A and B single electron transfer reactions, C disproportionation reaction).

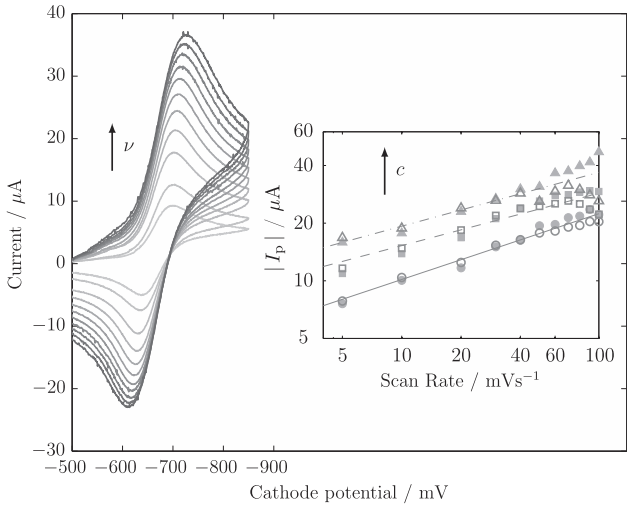

Fig. 5. Representative voltammograms corresponding to the micro cell (Fig. 1A) from 5 to 100 mV s^{-1} (5; 10; 20; 30; 40; 50; 60; 70; 80; 90; 100 mV s^{-1}) with a solution of 0.005 M $AQDS^{2-}$ in 0.1 M NaOH. Inset logarithmic plot shows the dependence of the peak currents with the scan rates and with $AQDS^{2-}$ concentration (▼ I_{pc} 0.015 M; ▽ I_{pa} 0.015 M; ■ I_{pc} 0.010 M; □ I_{pa} 0.010 M; ● I_{pc} 0.005 M; ○ I_{pa} 0.005 M).

with a 0.5 g mL^{-1} sodium-aluminium-silicate dispersion (Wessalith P, Degussa, Frankfurt, Germany), then rinsed in a 10 g L^{-1} nitric acid solution for 3 min and finally washed with deionised water. Spectrophotometric measurements were carried out with Specord S100 (Analytik Jena GmbH) UV/VIS Spectrophotometer, the absorption spectra were recorded in range of 450–800 nm and with an integration time of 80 ms, during 40 cycles at different scan rates 5 and 10 mV s^{-1} at 25 mV per cycle, under solutions of 0.005 M and 0.010 M $AQDS^{2-}$ in 0.1 M NaOH.

3. Results and discussion

3.1. Micro cell configuration

In alkaline solution e.g. 0.1 M NaOH, the sodium salt of the anthraquinone-1,5-disulfonic acid is present in full dissociated sulfonate form. This ion then is able to undergo a chemically reversible cathodic reduction to the corresponding 9,10-dihydroxy-anthraquinone-1,5-disulfonate, with both phenolic groups being fully dissociated. Thus compared to neutral or acid solution the overall reduction of $AQDS^{2-}$ in alkaline solution corresponds to a 2 e^- reduction, which no involvement of protonation steps (Fig. 4). The rather simple electrode reaction of this redox couple makes $AQDS^{2-}$ a useful system for the characterisation of the 3D-electrodes [9]. Sorption of the probe system on the synthetic fibre material used in the 3D-electrode can be neglected for several reasons: Strong repulsion is expected between the negatively charged probe molecule and the synthetic fibres which exhibit a negative zeta-potential at the strongly alkaline conditions applied. The experiments were performed below glass transition temperature of the polymers, thus access of sorbed molecules into the fibres is not possible. As the volume of catholyte used was high, stable concentration conditions were achieved. Thus no interference on the electron transfer reaction is expected due to low interactions between the synthetic materials used in the electrode and the probe molecule.

The $AQDS^{2-}$ redox system in alkaline solution was first studied by means of the micro cell configuration to determine the basic electrochemical behaviour of this system on Cu-electrodes (Fig. 1A). The micro cell configuration allows a scientific characterisation of the system. A fresh and uniform electrode surface is easier to prepare due to the small size of the cathode and less disturbing effects of convection allow better control of the mass transport to the electrode. The small dimensions of the working electrode and the absence of a cation-exchange membrane permits uniform current distribution on the cathode. Due to the low current density and the high conductivity in the electrolyte the ohmic drop in the electrolyte is negligible small. In addition the small volume of electrolyte permits the use of argon degassing to remove dissolved oxygen from the solution.

Fig. 5 shows representative voltammograms obtained with 0.005 M $AQDS^{2-}$ in 0.1 M NaOH using the micro cell at different scan rates. As expected, higher currents were obtained with increase of the scan rates and $AQDS^{2-}$ concentration. The response of the peak current with the scan rate is depicted in inset Fig. 5. For reversible redox systems (electron transfer kinetics faster than mass transport), the same anodic and cathodic peak currents are expected for all scan rates. As can be seen in Fig. 5, cathodic peak (I_{pc}) and anodic peak currents (I_{pa}) exhibit the almost same values at scan rates of 5–50 mV s^{-1}. Randles-Sevcik equation (Eq. (1)) can be used to describe the peak current response with the scan rate [10]:

$$I_p = \left(2.69 \cdot 10^5\right) n(\alpha n)^{1/2} A C_O D_O^{1/2} \nu^{1/2} \quad (1)$$

where n is the number of electrons involved in the process, α is the transfer coefficient, A is the cathode area in cm^2, C_O is the bulk concentration of the oxidised species in mol cm^{-3}, D_O is the diffusion coefficient of the oxidised species in cm^2 s^{-1} and ν is the scan rate in V s^{-1}. Thus data were fitted to an exponential function as $y = ax^b$ with a and b free parameters (inset Fig. 5). The results are presented in Table 2. All experimental data are listed in Tables A.1, A.2 and A.3 as Supplementary data. At higher $AQDS^{2-}$ concentrations difference between anodic and cathodic peak current increases, which also influences quality of the fitting. As expected from the Randles-Sevcik equation a direct relationship between a coefficients and $AQDS^{2-}$ concentration was observed, and all b values remained similar independent on $AQDS^{2-}$ concentrations. The calculated values for b deviate from theoretical value of 0.5 to smaller values, which points out the quasi-reversibility of the system. The dependence of the separation of the cathodic and anodic peak potential ($\Delta E_p = E_{pa} - E_{pc}$) with scan rates also supports the assumption of quasi-reversibility. Fig. 6A shows the response of the peak-to-peak potentials with scan rate and $AQDS^{2-}$ concentration

Table 2
Results of the exponential fitting for the peak current responses with the scan rates and $AQDS^{2-}$ concentrations obtained with the three different cells (± standard deviation).

Cell configuration	$AQDS^{2-}$ concentration/M	a/mA s^{-b} mV^{-b}	b	R^2
(A) Micro cell	0.005	$(4.6 \pm 0.8)\cdot 10^{-3}$	0.34 ± 0.04	0.95
	0.010	$(8.1 \pm 2.1)\cdot 10^{-3}$	0.27 ± 0.06	0.8
	0.015	$(10 \pm 4)\cdot 10^{-3}$	0.28 ± 0.10	0.7
Cell (B) Cu-plate WE	0.005	26 ± 6	0.27 ± 0.07	0.90
	0.010	47 ± 10	0.24 ± 0.07	0.90
	0.015	63 ± 14	0.20 ± 0.07	0.8
Cell (B) embroidered 3D WE	0.005	31 ± 6	0.29 ± 0.06	0.94
	0.010	54 ± 11	0.23 ± 0.06	0.90
	0.015	$(10 \pm 3)\cdot 10$	0.13 ± 0.11	0.5

determined using the micro cell. For reversible systems, ΔE_p is kept constant at all scan rates as $\Delta E_p = 59/n$ (mV), where n is the number of electrons involved in the process. In our case, an increase of ΔE_p with the scan rate is observed, confirming the quasi-reversibility of the system. For lower scan rates, a tendency to $\Delta E_p = 59$ mV, corresponding to $n = 1$, is observed. As seen in Fig. 4 the redox process from $AQDS^{2-}$ to $AQDS^{4-}$ is characterised by an overall two electron-transfer process. The experimental results indicate a consecutive two electron transfer reaction, which contains one single electron transfer as rate determining step. The first process would correspond to the formation of the radical anion ($AQDS^{\bullet 3-}$) followed by a second step, the formation of the fully reduced $AQDS^{4-}$. CV showed a single cathodic wave and no splitting of the cathodic wave occurs [11]. Most probably the formation of the radical anion by reduction of the $AQDS^{2-}$ through step A in Fig. 4 is the rate-determining process and $AQDS^{\bullet 3-}$ then undergoes rapid reduction according step B to the more stable fully reduced $AQDS^{4-}$ [12]. In addition a disproportionation of the $AQDS^{\bullet 3-}$ radical anion to $AQDS^{2-}$ and $AQDS^{4-}$ has to be considered as possible reaction pathway (reaction C in Fig. 4).

For quasi-reversible systems the standard heterogeneous electron transfer rate constant (k_0) can be determined from Fig. 6A following the analysis described by Nicholson for diffusion-controlled processes [13]. Nicholson defined a dimensionless kinetic parameter, Ψ, given by Eq. (2) if we consider transfer coefficients of 1/2 and the same diffusion coefficient for oxidised and reduced species,

$$\Psi = \frac{k_0}{(\pi D F \nu / RT)^{1/2}} \tag{2}$$

where D is the diffusion coefficient (in cm^2 s^{-1}), F the Faraday constant, R the gas constant (RT in mV), T the temperature (in K)

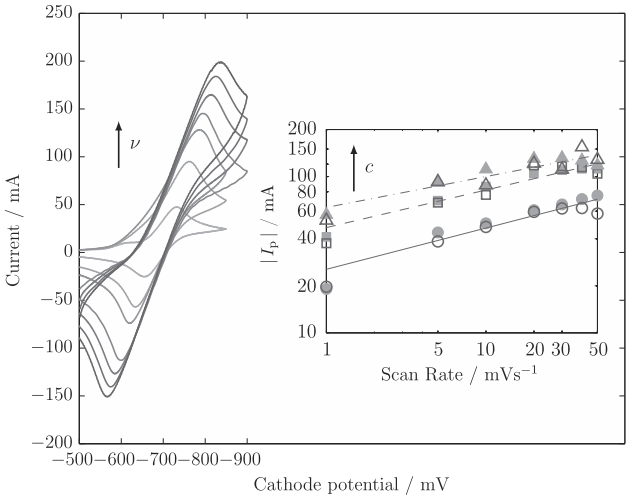

Fig. 7. Representative voltammograms using 100 cm^2 Cu-plate electrode at scan rates in the range 1–50 mV s^{-1} (1; 10; 20; 30; 40; 50 mV s^{-1}) at 0.010 M $AQDS^{2-}$ concentration. Dependence of the peak currents with the scan rates and $AQDS^{2-}$ concentrations (inset) (▼ I_{pc} 0.015 M; ▽ I_{pa} 0.015 M; ■ I_{pc} 0.010 M; □ I_{pa} 0.010 M; ● I_{pc} 0.005 M; ○ I_{pa} 0.005 M).

and ν the scan rate (in mV s^{-1}). Using the working curve from Nicholson, which shows the variation of the peak potential with Ψ, one can determine k_0 from the intersection of curves from Fig. 6B. Notice that k_0 is independent of the electrolyte concentration. Therefore, we considered the data where ΔE_p remained the same at different $AQDS^{2-}$ concentrations, at scan rates from 5 to 30 mV s^{-1}. Using a diffusion coefficient of $1.6\cdot 10^{-5}$ cm^2 s^{-1} [14], the calculated k_0 was $6.8\cdot 10^{-3}$ cm s^{-1}, which is in agreement with usual k_0 values for quasi-reversible systems [15].

The deviation from linearity in Fig. 5 at scan rates of 50 mV s^{-1} and higher indicates that the electrode reactions of the $AQDS^{2-}$ redox couple become more complicated as already indicated in Fig. 4. Above 50 mV s^{-1} the simplification of a simple one electron transfer step as rate determining reaction may be no longer valid.

3.2. 100 cm^2 Cu-plane electrode

The $AQDS^{2-}$ redox system was also studied using a 100 cm^2 Cu-plane electrode in a parallel plate geometry. In this cell the WE and the CE were separated by a cation ion exchange membrane. The geometric surface area of the cathode was $5.6\cdot 10^3$ times larger than the area of the circular Cu plane electrode (micro cell configuration). Representative current-potential responses using a 0.010 M

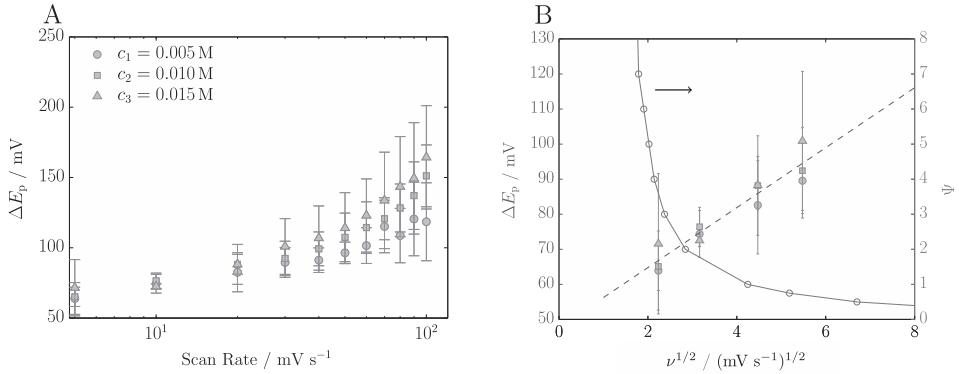

Fig. 6. Dependence of the peak potential separation with the scan rate and different $AQDS^{2-}$ concentrations c_1-c_3 using the micro cell (A). Curves for the determination of k_0 from the kinetic parameter Ψ defined by Nicholson [13] (B).

$AQDS^{2-}$ concentration are depicted in Fig. 7. As expected larger surface cathode areas provided higher current responses. The dependence of the peak current with the scan rate and $AQDS^{2-}$ concentration is shown in inset Fig. 7. Data was fitted to the same exponential function as above mentioned. Results are listed in Table 2. Similar *b* values were obtained for all the $AQDS^{2-}$ concentrations and *a* coefficients increased with $AQDS^{2-}$ concentrations. Coefficients from the best fits (0.005 M and 0.010 M $AQDS^{2-}$ concentration) of the micro cell and 100 cm^2 Cu-plane cell showed a relationship of $5.6–5.8 \cdot 10^3$ resembling the geometric surface area ratio between these two electrodes, in agreement with the proportional dependence of the area described by the Randles-Sevcik equation. Values of the power exponent *b* differed from the theoretical dependence 0.5 (not a diffusion-controlled process) but were very close to the *b* values obtained from the small cell. The results obtained with the plane electrode geometry demonstrate that the scale up of the electrode size by a factor of $5.6 \cdot 10^3$ and the use of a separator did not change the fundamental electrochemical conditions.

Fig. 8 shows the peak potential separation dependence with the scan rates and $AQDS^{2-}$ concentration. The peak-to-peak potential values at lower scan rates tended to $\Delta E_p = 59$ mV confirming consecutive two electron transfer reaction depicted in Fig. 4, since for a two electron transfer a $\Delta E_p = 59/2$ mV would be expected. Larger differences of the peak potential were obtained in comparison with the micro cell configuration. This shift of cathodic peak potentials to more negative values and anodic peak potentials to more positive values were caused by the common problems of scaling up a system, influence of position of ion-exchange membrane leading to deviation from ideal parallel plate geometry. The flexibility of the membrane separator thus can lead to differences in the ohmic drop in the electrolyte, which then broadens the current peaks due to the resistance polarization. Also convection effects in the cell can contribute to peak potential shifting, as the assumption of a fully reversible redox couple is not valid. As already shown the reduction of $AQDS^{2-}$ is a quasireversible electrode reaction and in addition the overall reduction is series of consecutive reactions (A, B and C in Fig. 4). This will lead to a shift of cathodic peak potential when migration effects will occur.

The parallel cell configuration and the $AQDS^{2-}$ system thus can be used as an instrumental set up to characterise Cu-based 3D-electrodes and compare the results with more simple geometries both in the same divided cell assembly and in relation to the miniaturised undivided cell.

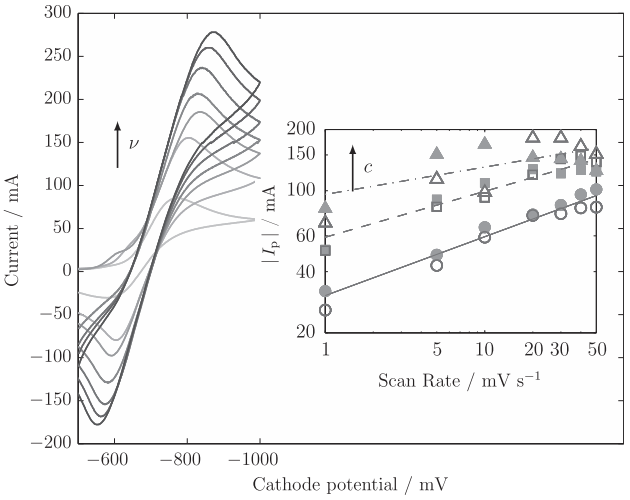

Fig. 9. Representative voltammograms obtained at 0.015 M $AQDS^{2-}$ concentration using 100 cm^2 embroidered Cu porous electrode. Inset figure shows the dependence of the peak currents with scan rates and $AQDS^{2-}$ concentration (▼ I_{pc} 0.015 M; ▽ I_{pa} 0.015 M; ■ I_{pc} 0.010 M; □ I_{pa} 0.010 M; ● I_{pc} 0.005 M; ○ I_{pa} 0.005 M).

3.3. Embroidered 3D Cu porous electrode

Dependent on the distance between embroidered Cu wires, porous 3D-electrodes with high surface area can be prepared. The surface area of an electrode is only dependent on the wire diameter and the density of wires mounted per unit volume of an electrode. In the present study a WE was prepared by embroidery of Cu-wires in such a way that a comparable surface area to the area of the plane Cu-electrode was obtained. This allows a more direct comparison of the different electrode concepts. The current-potential responses with scan rate at 0.015 M $AQDS^{2-}$ concentration are shown in Fig. 9. The peak currents with scan rate and $AQDS^{2-}$ concentration are represented in inset Fig. 9. The same exponential function as for the Cu-wire electrode and the plane electrode arrangement was fitted to the data. Akin results than those obtained with the 100 cm^2 Cu

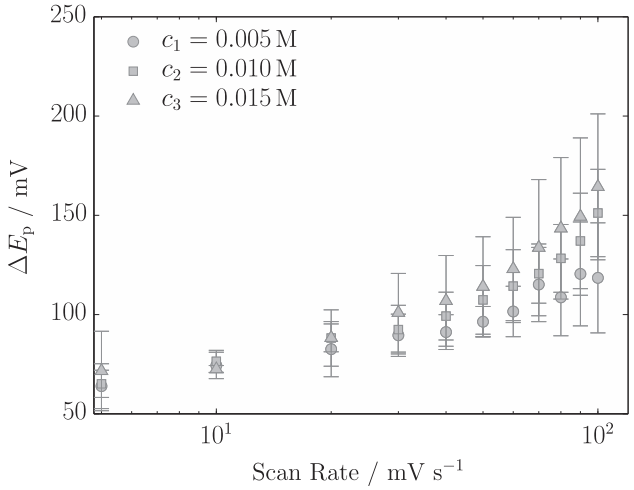

Fig. 8. Peak-to-peak potential separation using 100 cm^2 Cu-plate electrode with increasing the scan rate and $AQDS^{2-}$ concentrations.

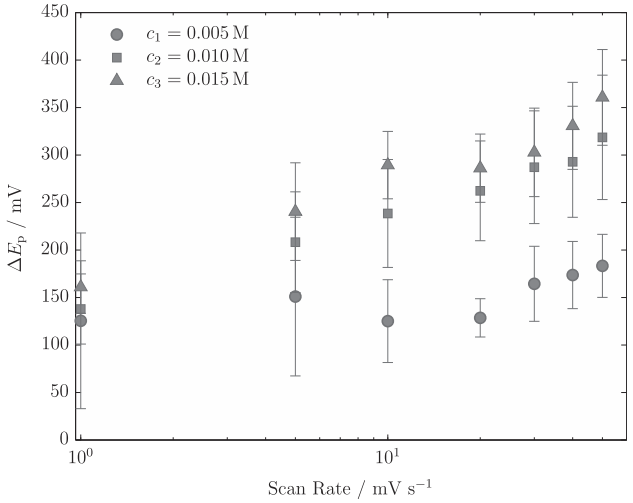

Fig. 10. Dependence of peak potential difference with scan rate using 100 cm^2 embroidered Cu porous electrode at different $AQDS^{2-}$ concentrations.

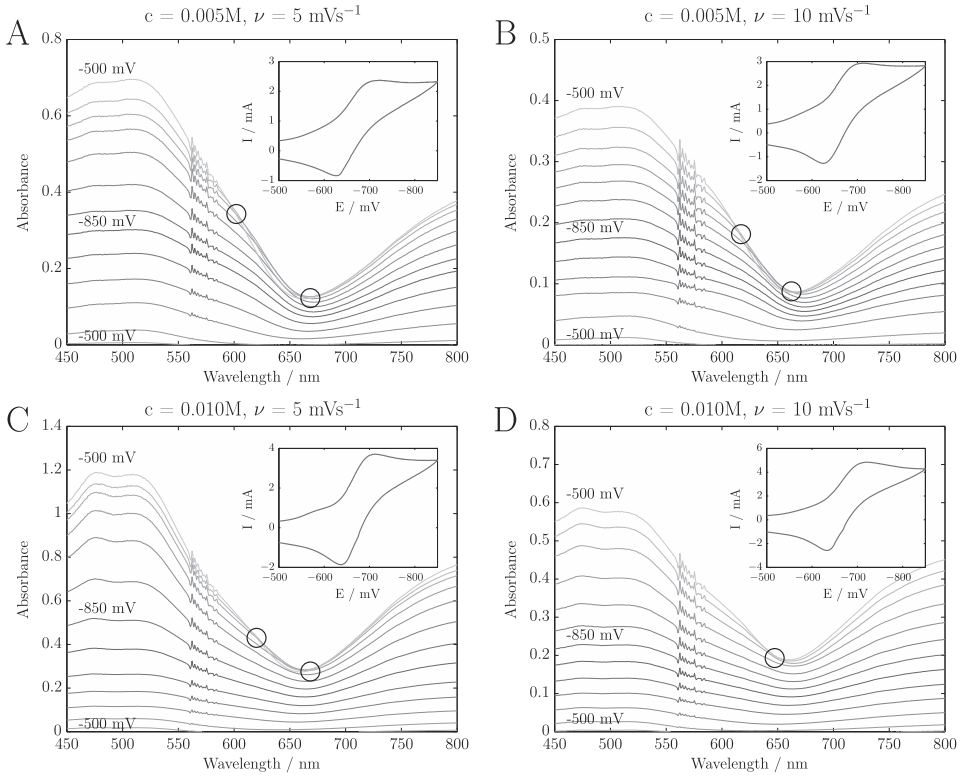

Fig. 11. Absorbance spectra while voltammograms were recorded using cell Fig. 1C at $AQDS^{2-}$ concentrations and scan rates: 0.005 M and 5 mV s^{-1} (A); 0.005 M and 10 mV s^{-1} (B); 0.010 M and 5 mV s^{-1} (C); 0.010 M and 10 mV s^{-1} (D).

plane electrode were found (see Table 2). The exponent of the scan rate, *b*, contains information about the mass transport at the electrode and one would expect a different value for the embroidered 3D Cu porous since a cylindrical diffusion is assumed. This effect becomes significant when the thickness of the diffusion layer exceeds the diameter of the Cu-wire (in this study 80 μm). Molina and coworkers [16] studied the behaviour of the diffusion layer thickness for reversible electrochemical processes considering different electrode geometries. Using their equations for the cylindrical geometry and sweep voltammetry for our experiments (diffusion coefficient of $1.6 \cdot 10^{-5}$ cm^2 s^{-1}), the estimated thickness of the diffusion layer is between 65 μm and 55 μm for the cathodic process at 1 mV s^{-1} and 50 mV s^{-1}, respectively. From these calculations, an assumption of linear diffusion is still in agreement with the response of 100 cm^2 Cu plane electrodes. Secondly, similar *a* values point out that the active area of the wire electrode is comparable to the plane electrode. In Table 1 the calculated surface area of the embroidered electrode was calculated with 100 cm^2, which confirms the calculated value for *a*. Fig. 10 shows the peak-to-peak potentials as a function of the scan rate and at different $AQDS^{2-}$ concentrations. Higher potential separations were observed in this cell configuration. The observations are characteristic of porous 3D-electrodes [17], which exhibit increasing active electrode depth with increasing electrode potential. As the reference electrode is positioned near the front of the electrode, the measured potential is related to this part of the electrode. With decreasing cathode potential a higher part of the porous structure participates in the electrode reaction. Apparently the inner part of the porous structure reduces $AQDS^{2-}$ at more negative potential, however this is due to the ohmic drop in electrolyte inside the porous structure, which thus shifts the respective peak potentials towards more negative values. In addition result the CV-peaks are broadened considerably.

It is important to mention that effects of convection in the 3D-electrode were neglected, which also could contribute to changes in the shape of the current peaks.

3.4. Spectroelectrochemical measurements

Spectroelectrochemical measurements were performed using cell configuration from Fig. 1C (Fig. 11). Series of absorbances spectra were obtained while voltammograms were run at scan rates of 5 and 10 mV s^{-1} and at 0.005 M and 0.010 M $AQDS^{2-}$ concentrations. Minimum absorption was obtained at a wavelength of 600 nm in agreement with the reddish colour of the reduced species ($AQDS^{4-}$).

In the spectra indication of one main component is given, which is the stable form of fully reduced $AQDS^{4-}$. The presence of $AQDS^{4-}$ in the diffusion layer still can be observed at the end of the anodic scan, independent on scan rate. There is indication of a second component through isosbestic points at 600 nm and 660 nm. The presence of the radical anion $AQDS^{\bullet 3-}$ which is continuously regenerated by cathodic reduction could explain the formation of isosbestic points, however, low probability of formation of higher concentrations of $AQDS^{\bullet 3-}$ in aqueous solution does not support this assumption. Here further detailed analysis would be required.

Similar to the quinone-hydroquinone system the formation of associated molecules could lead to changes in absorbance and could be used to explain the observed spectra. The disappearance of the isosbestic points at higher $AQDS^{2-}$ concentration and at higher scan rate does not support this explanation.

The spectra confirm a mechanism according to Fig. 4, in which one single electron transfer reaction is rate determining, as only one major species, $AQDS^{4-}$ is observed and under the experimental conditions used no significant amounts of intermediates could be detected.

4. Conclusions

For the development of electrochemical conversion and storage energy devices new electrode designs and cell performances are required. In this work the characterisation of 100 cm^2 embroidered Cu porous electrode is presented by means of the redox process of $AQDS^{2-}$ in alkaline solution with a micro cell and 100 cm^2 plane Cu-plate electrode. Cyclic voltammograms were recorded and the evolution of the peak currents and peak-to-peak potentials as a function of the scan rate and $AQDS^{2-}$ concentrations were studied.

Measurements from the micro cell allowed us to determine the standard heterogeneous electron transfer rate-determining constant for the $AQDS^{2-}$ redox process, $k_0 = 6.8 \cdot 10^{-3}$ cm s^{-1}, pointing out a quasi-reversible system. The tendency of the potential separation to 59 mV at low scan rates indicated that the redox process from $AQDS^{2-}$ to $AQDS^{4-}$ is characterised by consecutive two electron transfer reactions: one electron transfer from $AQDS^{2-}$ to the radical anion $AQDS^{\bullet 3-}$ with a disproportion to $AQDS^{4-}$, and another electron transfer from $AQDS^{\bullet 3-}$ to $AQDS^{4-}$.

Similar responses of the peak currents with scan rates were found for the three cell configurations, in agreement with the proportional ratio of their electrode areas, confirming the high efficiency of the embroidered 3D Cu porous electrode as a working electrode. The dependence followed the Randles-Sevcik equation showing a lower value for the scan rate exponent due to the quasi-reversibility of the system. For the embroidered 3D Cu porous electrode an increase of the peak-to-peak separation with scan rate was also observed due to the porous nature of the electrode. Notice that unlike the Cu-plane electrode, the embroidered 3D electrode allows customization of the electrode surface area by modifying the layout, number of Cu wires or Cu-wire diameters.

Common problems of scale-up a system such as convection, potential drop due to resistance polarization or migration effects were not considered. In addition followed-up chemical reactions, aggregates formation, copper oxidation and membrane effects were excluded.

Spectroelectrochemical measurements were also performed while cyclic voltammograms were recorded using a special cell with a plane Cu foil as a working electrode. Results showed that one single electron transfer reaction was rate determining in agreement with previous observations.

Acknowledgements

Authors thank Austrian Forschungsförderungsgesellschaft for funding Research Studio Austria - Smart Technical Embroideries RS-STE, Projekt Nr. 832003/RS-STE and the Smart Embroideries Group for providing electrode material samples.

Appendix A. Supplementary data

Supplementary data related to this article can be found at http://dx.doi.org/10.1016/j.jpowsour.2013.12.096

References

[1] M. Armand, J.M. Tarascon, Nature 451 (2008) 652–657, http://dx.doi.org/10.1038/451652a.
[2] Z. Gong, G. Zhang, S. Wang, J. Chem. 2013 (2013) 1–9, http://dx.doi.org/10.1155/2013/756307.
[3] R. Nissim, C. Batchelor-McAuley, Q. Li, R.G. Compton, J. Electroanal. Chem. 681 (2012) 44–48, http://dx.doi.org/10.1016/j.jelechem.2012.06.001.
[4] Y. Zhou, G. Zhang, J. Chen, G. Yuan, L. Xu, L. Liu, F. Yang, Electrochem. Commun. 22 (2012) 69–72, http://dx.doi.org/10.1016/j.elecom.2012.05.036.
[5] M. Weissmann, O. Crosnier, T. Brousse, D. Belanger, Electrochim. Acta 82 (2012) 250–256, http://dx.doi.org/10.1016/j.electacta.2012.05.130.
[6] L. Xie, L. Zhao, J. Wan, Z. Shao, F. Wang, S. Lv, J. Electrochem. Soc. 159 (2012) A499–A505, http://dx.doi.org/10.1149/2.112204jes.
[7] A.E. Murschell, W.H. Kan, V. Thangadurai, T.C. Sutherland, Phys. Chem. Chem. Phys. 14 (2012) 4626–4634, http://dx.doi.org/10.1039/c2cp23224c.
[8] G. Grabher, J. Hofer, M. Riedmann, T. Froeis, M. Lenninger, T. Bechtold, Elektrode für elektrochemische zelle, 2012, Austrian Patent Application AT20120822/24.08.2012.
[9] M. Lenninger, T. Froeis, M. Scheiderbauer, G. Grabher, T. Bechtold, J. Solid State Electrochem. 17 (8) (2013) 2303–2309, http://dx.doi.org/10.1007/s10008-013-2108-1.
[10] V.S. Rao, Polarography and Allied Techniques, Universities Press, 2002.
[11] S. Bailey, I. Ritchie, Electrochim. Acta 30 (1985) 3–12, http://dx.doi.org/10.1016/0013-4686(85)80051-7.
[12] A.J. Bard, L.R. Faulkner, Electrochemical Methods: Fundamentals and Applications, Wiley, 2000.
[13] R.S. Nicholson, Anal. Chem. 37 (1965) 1351–1355, http://dx.doi.org/10.1021/ac60230a016.
[14] J. Katsumi, T. Nakayama, Y. Esaka, B. Uno, Anal. Sci. 28 (2012) 257–265, http://dx.doi.org/10.2116/analsci.28.197.
[15] G.A. Mabbott, J. Chem. Educ. 60 (1983) 697, http://dx.doi.org/10.1021/ed060p697.
[16] A. Molina, J. Gonzalez, F. Martinez-Ortiz, R.G. Compton, J. Phys. Chem. C. 114 (2010) 4093–4099, http://dx.doi.org/10.1021/jp9115172.
[17] J. Newman, C. Tobias, J. Electrochem. Soc. 109 (1962) 1183–1191, http://dx.doi.org/10.1149/1.2425269.